PHARMACIA

Pharmacia 71: 1–10
DOI 10.3897/pharmacia.71.e127826

Research Article

Freeze-dried erythromycin nanocrystals: preparation, characterisation, antimicrobial activity, and aerodynamic properties

Juhaina M. Abu Ershaid[1], Suha M. Abudoleh[2], Dima N. Lafi[1]

1 *Department of Applied Pharmaceutical Sciences and Clinical Pharmacy, Faculty of Pharmacy, Isra University, Amman 11622, Jordan*
2 *Department of Basic Pharmaceutical Sciences, Faculty of Pharmacy, Middle East University, Amman 11831, Jordan*

Corresponding author: Juhaina M. Abu Ershaid (Juhaina.abuershaid@iu.edu.jo)

Received 18 May 2024 ♦ **Accepted** 5 August 2024 ♦ **Published** 27 August 2024

Citation: Abu Ershaid JM, Abudoleh SM, Lafi DN (2024) Freeze-dried erythromycin nanocrystals: preparation, characterisation, antimicrobial activity, and aerodynamic properties. Pharmacia 71: 1–10. https://doi.org/10.3897/pharmacia.71.e127826

Abstract

Background: This study aims to present the development and evaluation of freeze-dried erythromycin nanocrystals to enhance the solubility, dissolution rate, and antibacterial potency of erythromycin.

Results: Erythromycin nanocrystals had a particle size of 239.3 ± 24.6 nm with 0.17 ± 0.01 PDI. Erythromycin nanocrystals had significantly higher saturation solubility and a faster dissolution rate compared to coarse erythromycin. Nanocrystals showed a high drug content of 92.69% ± 2.82, while the aerodynamic characteristics demonstrated an emitted dose (ED%) of 83.68% ± 5.32 with a mass median aerodynamic diameter of 2.13 µm. Around half reduction of the minimum inhibitory concentrations were observed against *P. aeruginosa* and *E. coli* (125 µg and 62.5 µg, respectively).

Conclusion: The nanocrystal formulation of erythromycin presented in this study holds promise as an innovative approach to enhance the solubility, dissolution rate, and antibacterial activity of erythromycin for effective pulmonary administration.

Graphical abstract

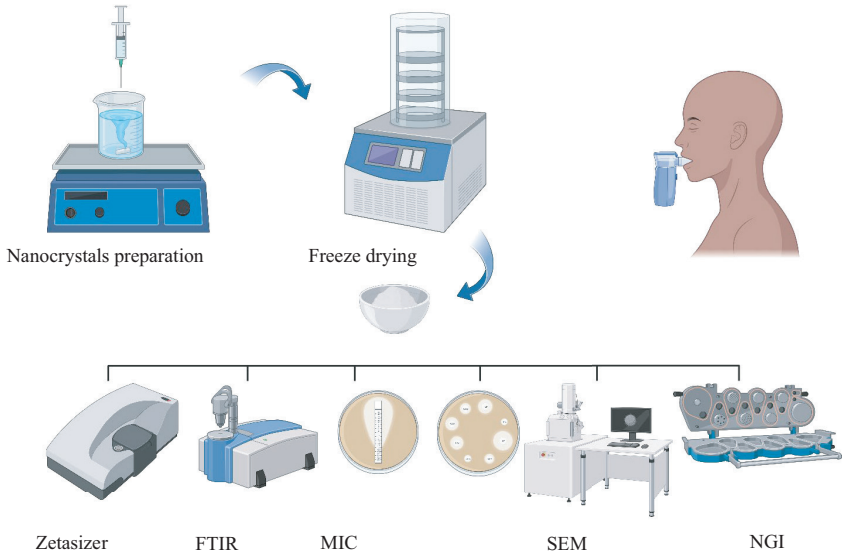

Keywords

Antibiotics, freeze dryer, infections, lung, nanotechnology, NGI, and MIC.

Introduction

Erythromycin is one of the macrolide antibiotics commonly prescribed for several bacterial infections, including pulmonary infections (Hoyt and Robbins 2001; Essack et al. 2019) Erythromycin works by inhibiting the synthesis of protein in the bacteria, which causes an inhibition of the bacterial replication and growth (Francino, 2016). It is a wide-spectrum antibiotic that works on gram-negative and gram-positive bacteria (Fan et al. 2009). Despite its widespread use, erythromycin has significant limitations that reduce its therapeutic effectiveness. These include its hydrophobic nature, poor aqueous solubility, and instability in acidic gastric environments (Wang et al. 2006). Upon oral administration, erythromycin highly degrades in the gastric medium, which reduces the oral bioavailability. Additionally, erythromycin causes liver toxicity and gastrointestinal side effects due to its chemical conversion in an acidic medium (Carter et al. 1987). Oral erythromycin has an unacceptable taste, which reduces children's acceptance and adherence. Also, it induces high gut motility, which cannot be tolerated by elderly patients (Dave et al. 2012).

Upon oral administration, erythromycin highly distributes around the human body, which leads to untargeted site exposure and adverse effects (Kanfer et al. 1998). This wide distribution increases the risk of developing bacterial resistance in addition to systemic toxicity (Gyselinck and Janssens 2024).

These drawbacks of erythromycin induced an urgent need to develop novel formulations of erythromycin, especially with the accelerated bacterial resistance to the current antibiotics while reaching a plateau in developing new ones. Therefore, lowering the effective antibiotic dose by enhancing the antibiotic's solubility and potency has become a priority (Platon et al. 2022).

Delivering antibiotics *via* pulmonary inhalation showed superior therapeutic outcomes for several lung infections, including cystic fibrosis (CF), bronchitis, and chronic obstructive pulmonary disease (COPD) (Patton and Byron 2007; Mansour et al. 2009). However, the efficient delivery of antibiotics *via* this route is limited by their poor solubility, particle size, and challenging features of the lung (Ling et al. 2014; Loira-Pastoriza et al. 2014). Nanoformulations overcome several drug delivery challenges by enhancing solubility, reducing particle size, and increasing the retention time in the lungs (Elsayed and AbouGhaly 2016; Mangal et al. 2017). Nanocrystals, a free polymer nanoformulation, gained significant attention for pulmonary delivery of poorly soluble drugs (Khatib et al. 2019). The high drug content of this formulation is due to the minimal use of excipients (Yue et al. 2022). This technology offers reducing the size to the nanoscale, increasing the surface area, and enhancing drug solubility and dissolution rate (Cheshmehnoor et al. 2023). Nanocrystals have been previously investigated for delivering antibiotics for pulmonary infections (He et al. 2020). This formulation enhances the solubility of antibiotics and ultimately enhances their efficient delivery (Gigliobianco et al. 2018; Khatib et al. 2019). In order to enhance the solubility and saturation solubility of erythromycin, nanocrystal erythromycin was formulated in this work. Further, nanocrystal erythromycin was characterised in terms of size, PDI, Zeta potential, morphology, drug content, solubility, *in vitro* release, antibacterial activity, and aerodynamic performance. These studies were carried out to evaluate the potential enhancement of erythromycin solubility, dissolution rate, and antibacterial activity and to investigate the suitability of this formulation for pulmonary administration.

Materials and methods

Materials

Erythromycin was obtained from Dar Al Dawa® (Jordan), sodium lauryl sulphate and mannitol were obtained from S&C Chemicals® (Jordan), and phosphate buffer saline was obtained from OXOID® (England). All other reagents were used in analytical grade. Tween® 80 was obtained from BBC Chemical for Labs (Jordan). For antibacterial activity testing, *B. cereus* (ATCC 11778), *S. aureus* (ATCC 9144), *E. coli* (ATCC 25922), *P. aeruginosa* (ATCC 9027), and nutrient broth and agar (Oxoid, England) were used.

Methods

Erythromycin nanocrystal preparation and lyophilisation

Erythromycin nanocrystals were prepared using the antisolvent nanoprecipitation method (Liu et al. 2020). Erythromycin powder (500 mg) was dissolved in 10 ml of ethanol and placed in a sonicater until full dissolution was achieved. In a glass beaker, 30 ml of 0.5% (w/v) sodium lauryl sulphate (SDS) in phosphate buffer solution (PBS) was prepared. Erythromycin solution was added to the aqueous solution under magnetic stirring of 300 rounds per minute (rpm). To obtain a dry powder suitable for inhalation, 2% w/w mannitol was added to the nanocrystal's solution as a cryoprotectant for the lyophilization

process. The solution was poured into four falcon tubes (15 ml) and pre-frozen using a deep freezer (Ultra Low Temperature Freezer, Haier® Biomedical) at -70 °C for 4 hours, then samples were freeze-dried using a freeze dryer (Heto FD1.0, Heto-Holten®, Denmark) at -90 °C and 380 mT of pressure for 12 hours to yield dry nanocrystals in powder form. Fig. 1 briefly illustrates the preparation and lyophilization of erythromycin nanocrystals.

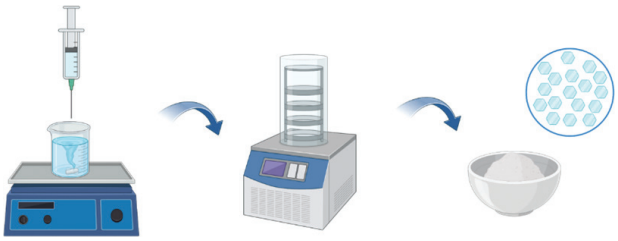

Figure 1. Graphical illustration of the anti-solvent nanoprecipitation method and freeze-drying lyophilisation used to prepare erythromycin nanocrystals.

Erythromycin nanocrystals characterisation

Erythromycin nanocrystals were characterised in terms of particle size, polydispersity index (PDI), and zeta potential using a Zetasizer Nano ZS-90 instrument (Malvern® Instruments, Malvern, UK). An aliquot of the lyophilised nanocrystal solution was diluted in distilled water before the measurement. Measurements were performed in triplicate using a 90° scattering angle at 25 °C. The same method was applied to coarse erythromycin to compare the size of unmodified erythromycin and erythromycin nanocrystals. The displayed results are the average value ± standard deviation (SD). A scanning electron microscope (SEM) was used to visualise the freeze-dried nanocrystal powder. The powder was distributed on an SEM stub and sputtered with graphite.

Drug content

Erythromycin content in nanocrystals was estimated according to the following method. Briefly, 50 mg of erythromycin nanocrystals was weighed precisely and dissolved in ethanol. The samples were then centrifuged at 10,000 g for 10 min. The supernatant (to quantify free erythromycin) was diluted and analysed using an ultraviolet (UV)-spectrophotometer at 280 nm wavelength. The calibration curve was conducted over a concentration range of 1.56–25 mg/ml. The drug content was determined according to the below Equation 1. The calibration method was used to quantify erythromycin in the formulation; the R-value was 0.999, and the data is presented as mean ± SD.

$$Erythromycin\ \ content\,\% = \frac{\text{Erythromycin mass}}{\text{Total mass of the formulation}} * 100\% \quad \text{Equation 1}$$

Fourier transform infrared spectroscopy

Fourier transform infrared (FTIR) spectra were obtained with an FTIR spectrometer (PerkinElmer®, USA) in the 4000–400 cm^1 spectral domain with a resolution of 4 cm^{-1}. The FTIR spectrum of erythromycin nanocrystals was compared to erythromycin coarse drug spectrum, and functional groups were determined.

Saturation solubility study

The saturation solubilities of coarse erythromycin and erythromycin nanocrystals were evaluated using the Higuchi method (Jiang et al. 2012). An excess amount of coarse erythromycin and erythromycin nanocrystals were each added to 5 ml of phosphate buffer (PBS) (pH=7.4). Samples were kept at 37 ± 0.5 °C under continuous shaking of 80 rpm for 48 h. During analysis, 1 ml of each sample was taken, centrifuged at 1000 × g for 10 min, and diluted. Analysis was performed using a UV-spectrophotometer at a lambda max of 280 nm. The experiments were conducted in triplicate, and the data were presented as mean ± SD.

In vitro release study

The *in vitro* release of nanocrystals was evaluated using dialysis methods. Approximately 5 mg of erythromycin and an amount of nanocrystal corresponding to 5 mg erythromycin were each placed in the dialysis membrane (12K MW). The release was performed in 100 ml release media of phosphate buffer (PBS) (pH=7.4) with 2.0% (w/v) Tween 80. Samples were kept under continuous agitation of 80 rpm at 37 ± 0.5 °C. At predetermined time points (5, 10, 20, 30, 60, 90, 180 min), 1 ml of the samples was withdrawn and centrifuged at 1000 × g for 10 min. Erythromycin content in the supernatant was analysed by UV-spectroscopy. An equal volume of fresh medium was added to the release medium to maintain sink condition. The experiment was run in triplicate, and the data were presented as mean ± SD.

Agar well diffusion method

The inhibition zones of erythromycin and erythromycin nanocrystals were determined according to Balouiri et al. 2016 (Balouiri et al. 2016). Shortly, 0.5 McFarland of each bacterial strain was prepared, and 100 µl of bacteria were spread evenly over the surface of nutrient agar (Balouiri et al. 2016). Agar wells were prepared with diameter 8 mm. Each well was filled with 200 µl of erythromycin (1 mg/ml) and erythromycin nanocrystal (1 mg/ml) and 0.5% (w/v) SDS in PBS as a control. The plates were incubated at 37 °C for 18 h. Inhibition zones were measured using a ruler to record the results in cm. The experiment was repeated three times.

The minimum inhibitory concentration (MIC)

The MIC was tested according to the method of Balouiri et al. 2016 using the 96-well plate method (Balouiri et al. 2016). Shortly, 100 µl of nutrient broth were added to each well. One hundred microlitres of each erythromycin and erythromycin nanocrystal were added separately to the first well and serially diluted as follows: (100 µg, 500 µg, 250 µg, 125 µg, 62.5 µg, 31.25 µg, 15.625 µg, 7.8µg, 3.9 µg, and 1.95 µg). One hundred microlitres of 1×10^6 CFU/ml bacteria were added to each well. Negative control was

treated with PBS only. The plates were incubated at 37 °C for 18 h. The MIC was recorded as the lowest concentration of treatment with no visible growth.

Aerodynamic characteristics of erythromycin nanocrystals using a next-generation impactor (NGI)

The aerodynamic deposition and distribution of erythromycin nanocrystals were analysed using NGI (Copley Scientific Limited, Nottingham, UK). NGI is a multi-stage impactor recommended by the European Pharmacopeia (EP) and the United States Pharmacopeia (USP) for aerodynamic evaluation of dry powder inhalers (Marple et al. 2003). NGI has seven stages varying in hole diameter from 14.3 mm to 0.206 mm in addition to a micro-orifice collector (MOC) with 70 µm hole diameter. For each stage, particles are deposited in a collection cup, which is held in a tray. To prevent powder from bouncing back, trays were treated with 1% v/v glycerine in an acetone solution and left to dry. Erythromycin nanocrystals were encapsulated in size three gelatine capsules; 6 capsules were used for each run. Each capsule contained approximately 20 mg (±10%) of the nanocrystals. The air flow rate was maintained at 60 L/min for a duration of 4 seconds, resulting in a total air volume of 4 L. NGI has 8 trays with different orifice sizes to mimic the pulmonary to disperse the nanocrystals. The filled capsules were introduced into an Aerolizer® actuation device as shown below in Fig. 2**.** Upon puncturing the capsules, the nanocrystals were aerosolised into the NGI. The quantity of nanocrystals collected in each tray was determined by dissolving the fluffy powder in 10 ml of ethanol. Subsequently, the samples were vortexed, then centrifugated at 10,000 g for 10 minutes. The erythromycin content was assessed using UV spectroscopy at a wavelength of 248 nm. Aerodynamic evaluation was based on respirable dose (RD), emitted dose (ED), and fine particle fraction (FPF). As detailed below in Equations 2, 3, and 4, RD is known to be the total amount of deposited powder in trays 2 to 7. The emitted dose percent (ED%) is the total deposited amount in all stages (trays 1 to 8) divided by the total dose of powder, the induction tube, and the pre-separator. The FPF of the emitted dose (FPF-ED) was calculated by dividing the RD by the emitted dose (Al-Tarawneh et al. 2022). According to the British Pharmacopeia (BP), mass median aerodynamic diameter (MMAD) represents the particle size, which 50% of the particles lie below on the basis of mass. This value was obtained by plotting the cut-off diameter of NGI trays against the cumulative mass of erythromycin nanocrystals (Khatib et al. 2019). Measurements were recorded in triplicates and reported as mean ± SD.

$$RD = \sum_{t=2}^{7} m \qquad \text{Equation 2}$$

$$ED\% = \frac{\sum_{t=1}^{8} m}{total\ \ dose\ \ of\ \ powder} \qquad \text{Equation 3}$$

$$FPF - ED = \frac{RD}{ED} \qquad \text{Equation 4}$$

RD: Respirable dose
m: erythromycin mass (mg)
t: Tray of the next generation impactor (NGI)
ED%: Emitted Dose Percent
FPF: Fine Particle Fraction

Statistical analysis

All data were expressed as the means ± SDs, calculated using Microsoft Office 365 Pro Plus Excel® (Microsoft Corporation, Redmond, WA, USA). Where appropriate, t-test was used for the comparison of two groups. A one-way ANOVA was used for the comparison of multiple groups. In all cases, P <0.05 was considered a significant difference.

Results

Erythromycin nanocrystals characterisation

As outlined below in Table 1, the prepared nanocrystals in this work had a particle size of 239.3 ± 24.6 nm with 0.17 ± 0.01 PDI. The zeta potential of the nanocrystals was measured to be -39.5 ± 2.3. Corse erythromycin size was also measured using exactly the same method used for the nanocrystals. Neat erythromycin had a particle size of 25.06 ± 5.92 µm. Results revealed a significant difference in particle size between erythromycin and erythromycin nanocrystals (P value = 0.0057). Fig. 3 shows the morphology of the lyophilised freeze-dried nanocrystal powder. SEM images were taken at different magnifications. At high magnification (35000 ×), images revealed that nanocrystals were in the nanoscale and demonstrated a uniform shape.

Table 1. Characterisation of erythromycin nanocrystals, including size, polydispersity index, zeta potential, and drug content.

Size	Loading Capacity	Zeta Potential	PDI
239.3 ± 24.6 nm	92.69% ± 2.82	-39.5 ± 2.3 mV	0.17 ± 0.01

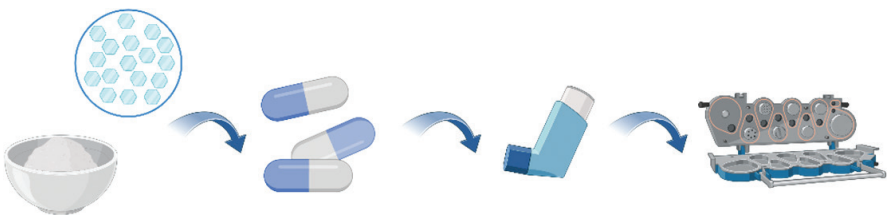

Figure 2. Graphical illustration shows the *in vitro* aerodynamic evaluation of erythromycin nanocrystals using a next-generation impactor.

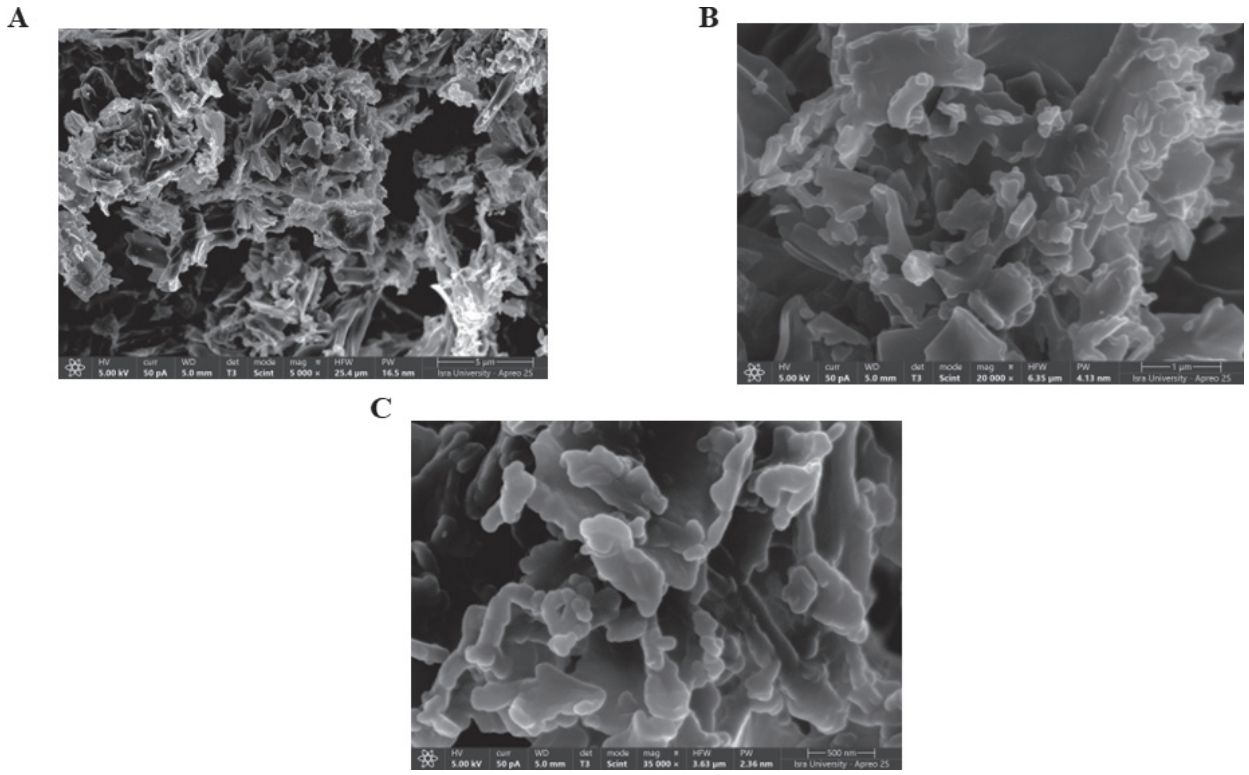

Figure 3. Scanning electron microscope images (SEM) showing the freeze-dried erythromycin nanocrystal powder at different magnifications **A.** At 5000 ×; **B.** At 20000 ×; **C.** At 35000 ×.

Drug content

Erythromycin nanocrystals were successfully prepared using the antisolvent nanoprecipitation method, resulting in a uniform structure and size to prevent agglomeration (Yue et al. 2022). In this work, the erythromycin content in the lyophilised nanocrystals was estimated using UV spectroscopy. Lyophilised nanocrystals showed drug content of 92.69% ± 2.82. Nanocrystal formulations are known to have a high drug content percent, as reported previously (Liu et al. 2010).

Fourier transform infrared spectroscopy

FTIR spectra of erythromycin and nanocrystals were obtained and compared as shown in Fig. 4, Table 2. It was found that the main functional groups of erythromycins, including the $N(CH3)_2$ vibration band, appear at 1455 cm^{-1}, the sharp band at 2975 cm^{-1} can be assigned to CH_2 stretching vibration modes, and the band at 3466 cm^{-1} is assigned to OH stretching modes. Besides, the carbonyl group shows strong bands at 1733 and at 1378 cm^{-1}.

Saturation solubility study

Saturation solubility of erythromycin nanocrystals was evaluated and compared to coarse erythromycin. As detailed in Fig. 5, nanocrystals showed a saturation solubility of 3.36 ± 0.1 mg/ml, whereas coarse erythromycin had a solubility of 0.47 ± 0.13 mg/ml. Nanocrystallisation of erythromycin resulted in an enhancement of the saturation solubility as there was a significant difference between the two solubilities (P value < 0.0001).

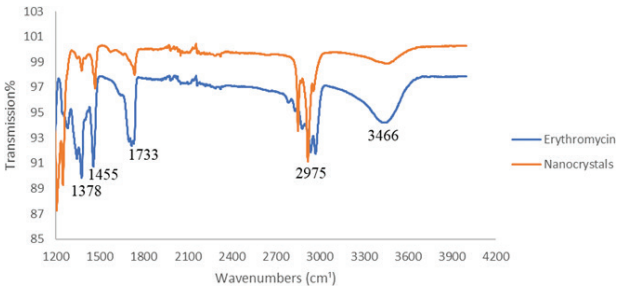

Figure 4. Fourier transform infrared spectrum of erythromycin and erythromycin nanocrystals.

Table 2. The main functional groups of erythromycins and their absorption wavelengths.

Erythromycin Functional Groups	Erythromycin Nanocrystals Functional Groups	Absorption Wavelength (cm^{-1})
Hydroxyl (-OH)	Hydroxyl (-OH)	3466
Methoxy ($-OCH_3$)	Methoxy ($-OCH_3$)	2975
Keto (-C=O)	Keto (-C=O)	1733
Amino ($-NH_2$)	Amino ($-NH_2$)	1455
Dimethylamino ($-N(CH_3)_2$)	Dimethylamino ($-N(CH_3)_2$)	1387

In vitro release study

In this study, the dissolution rates of erythromycin and erythromycin nanocrystals were investigated.

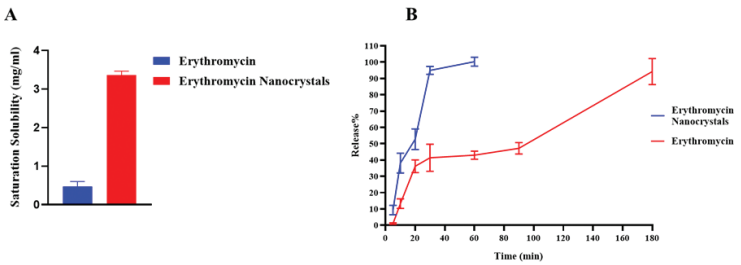

Figure 5. A. Saturation solubility study of erythromycin and erythromycin nanocrystals; **B.** The *in vitro* release profile of erythromycin nanocrystals and coarse erythromycin.

As illustrated in Fig. 5, the release rate of nanocrystals was faster than coarse erythromycin. Around 60 min were required to release 100% of the nanocrystals, whereas 180 min were required for complete coarse erythromycin release. At the first 5 min, 9.3% ± 2.33 of the nanocrystals were released compared to only 0.98% ± 0.47 of coarse erythromycin. This difference in the release profile continued throughout the experiment; at 10 min, 38.11% ± 6.07 of nanocrystals were released, while 13.25% ± 2.9 of coarse erythromycin were released. For nanocrystals, approximate 50% release was accomplished at 20 min, whereas coarse erythromycin took around 90 min to release the same percent. Nanocrystals with their small size and high surface area exhibit an enhancement of the dissolution rate of therapeutics, as demonstrated in previous studies (Müller et al. 2011).

Agar well diffusion method

The vehicle used in this experiment was PBS, which didn't show any activity against any of the tested bacteria. The difference between the activity of erythromycin and the nanocrystal preparation was insignificant using the agar well diffusion method, as detailed in Table 3.

Table 3. The inhibition zone of erythromycin and erythromycin nanocrystals against tested bacteria; the diameter was reported in cm ± SD, *n*=3.

Sample	*B. cereus* (*ATCC 11778*)	*S. aureus* (*ATCC 9144*)	*E. coli* (*ATCC 25922*)	*P. aeruginosa* (*ATCC 9027*)
PBS	No activity	No activity	No activity	No activity
Erythromycin (1 mg/ml)	3.8 ± 0.05	2.7 ± 0.08	2.4 ± 0.05	2.4 ± 0.05
Nanocrystals (1 mg/ml)	3.6 ± 0.08	2.5 ± 0.08	2.3 ± 0.05	2.1 ± 0.2

Minimum inhibitory concentration

The results of MIC values showed a significant reduction in the MIC values against Gram negative bacteria tested in this study, where the MIC value reduced when using the nanocrystal preparation of erythromycin from 250 µg to 125 µg against *P. aeruginosa* as shown in Table 4. In the case of *E.coli* the MIC value reduced from 125 µg to 62.5 µg. No change in the MIC values was recorded against *B. cereus* or *S. aureus*.

Table 4. The MIC values of erythromycin and erythromycin nanocrystal against tested bacteria.

Sample	*B. cereus* (*ATCC 11778*)	*S. aureus* (*ATCC 9144*)	*E. coli* (*ATCC 25922*)	*P. aeruginosa* (*ATCC 9027*)
PBS	No activity	No activity	No activity	No activity
Erythromycin (1 mg/ml)	0.5 µg/ml	<0.5 µg/ml	125 µg/ml	250 µg/ml
Nanocrystals (1 mg/ml)	0.5 µg/ml	<0.5 µg/ml	62.5 µg/ml	125 µg/ml

Aerodynamic characteristics of erythromycin nanocrystals using a next-generation impactor (NGI)

Freeze-dried erythromycin nanocrystals were light, fluffy powder. The aerodynamic characteristics of the nanocrystals were evaluated using NGI as detailed in Table 5. Fig. 6 shows the deposition of erythromycin nanocrystals among NGI trays. The RD was evaluated to be 16.37 ± 3.84 mg, whereas the ED% was determined by dividing the cumulative drug from all stages over the theoretical dose. Erythromycin nanocrystals had an ED% of 83.68% ± 5.32. MMAD was found to be 2.13 µm indicating the high probability of erythromycin nanocrystals to reach the lower respiratory system (Pandey and Ahmad 2011; Abadelah et al. 2020; Asha et al. 2023). Nanocrystals showed FPF-ED% of 9.77% ± 2.3.

Table 5. The aerodynamic characteristics of erythromycin nanocrystals.

RD	ED%	FPF-ED	MMAD
16.37 ± 3.84 mg	83.68% ± 5.32	9.77% ± 2.3	2.13 µm

Discussion

Erythromycin nanocrystals were prepared using the bottom-up method in a process known as antisolvent nanoprecipitation. This method provides a uniform structure and size of the nanocrystals to ensure stability and avoid agglomeration (YUE et al. 2018). Further, nanocrystals were lyophilised using the freeze-drying process. This process includes removing solvent by freezing followed by sublimation (Siow et al. 2018). This formulation allows the formation of nanoscale crystals with minimum use of excipients (Xiang et al. 2022). In this work, erythromycin nanocrystals had a drug content of 92.69% ± 2.82. Previous studies on nanocrystals reported similar high drug content due to the low percentages of other ingredients (Liu et al.

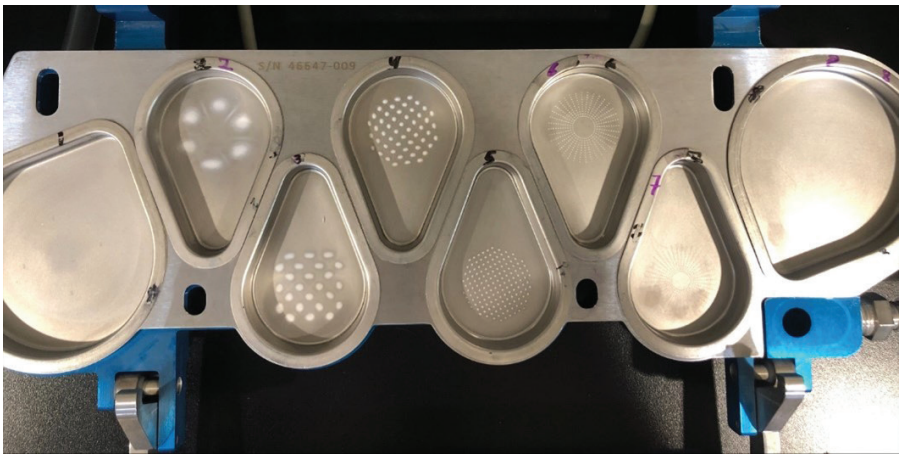

Figure 6. Image showing the deposition and distribution of erythromycin nanocrystals among next-generation impactor trays.

2010). The high erythromycin content in nanocrystals gives an advantage to this formulation over other erythromycin formulations. It was reported that erythromycin polymeric microspheres had a drug content of 22%, while erythromycin liposomes yielded a drug content of 7.3% ± 0.2 (Park et al. 2015; Bennabi et al. 2022). Additionally, erythromycin nanocrystals showed a narrow size distribution, as the PDI value was 0.17 ± 0.01 PDI. The PDI value can be used to evaluate the physical stability of the nanocrystals. The lower the PDI, the higher the physical stability of the formulation (Jin et al. 2019). Erythromycin nanocrystals demonstrated a zeta potential value of -39.5 ± 2.3. Zeta potential is commonly measured to estimate the stability of the formulation (Kulshreshtha et al. 2009). This value measures the surface charge of the particles. The higher the charge, the higher the electrostatic repulsion and the higher the stability (Bhadra et al. 2016). FTIR was used to assess any possible interaction between erythromycin and other excipients. All the functional groups in erythromycin were detected in erythromycin nanocrystals. These findings indicated the absence of any chemical interaction between erythromycin and the other used excipients in the nanocrystal formulation (Abareshi et al. 2021). In general, nanocrystal formulations are known to enhance the solubility and dissolution rate of therapeutics. A saturation solubility study was performed to evaluate the solubility enhancement of erythromycin. Nanocrystal erythromycin had a saturation solubility of 3.36 ± 0.1 mg/ml compared to 0.47 ± 0.13 mg/ml of coarse erythromycin. This significant enhancement of solubility can be explained due to size reduction and enlargement of the surface area. This finding is in parallel with previously reported nanocrystals of flurbiprofen, a poorly aqueous soluble drug (Mushtaq et al. 2024). Nanocrystallisation of flurbiprofen significantly enhanced the water solubility of the drug, which consequently enhanced the bioavailability. Moreover, in our study, the *in vitro* dissolution study of erythromycin nanocrystals was carried out and compared to the *in vitro* dissolution of coarse erythromycin. The two release profiles were obtained under the same conditions to ensure realistic comparison. Tween®80 was added to the release media to mimic the presence of surfactants in the alveoli and airway tract (Kim et al. 2016). The *in vitro* release study indicated an enhancement in the dissolution profile of erythromycin upon nanocrystallisation. Nanocrystals had a 100% release within 60 min, whereas coarse erythromycin required 180 min for complete release. Further, during the first 5 min, nanocrystals and coarse erythromycin had a release percent of 9.3% ± 2.33 and 0.98% ± 0.47 respectively. These findings support the role of nanocrystal formulation in enhancing the dissolution profile for poorly water-soluble drugs (Pelikh et al. 2021). Nanocrystals were applied to nintedanib to enhance their dissolution profile and eventually enhance bioavailability (Zhu et al. 2022).

Erythromycin as macrolides was used as a treatment against Gram-positive and Gram-negative bacteria with certain drawbacks of its activity. The main cause of mortality in cystic fibrosis (CF) cases are chronic pulmonary infections caused by *Pseudomonas aeruginosa* (Heijerman, 2005). *P. aeruginosa*, commonly found in soil and aquatic settings, is frequently acquired by CF patients from their immediate surroundings (Lozano-Iturbe et al. 2024). Initially, CF patients tend to encounter this bacterium from their local environments (Jin, 2024). However, infection with epidemic *P. aeruginosa* strains typically emerges later in the progression of CF lung disease. As individuals with CF age, the prevalence of *P. aeruginosa* infection rises, often displacing early non-*Pseudomonas* airway colonisers (Parkins et al. 2018). Controlling and eradicating *P. aeruginosa* poses significant challenges compared to other pathogens due to its high resistance to a wide array of antibiotics and its tendency to form biofilms (Liu et al. 2024). These biofilm infections are marked by reduced susceptibility to antibiotics and a formidable resistance to the host's immune response (Kar et al. 2024). The result of this study was consistent with other studies prepared the erythromycin as nanoformulation with different pharmaceutical preparations as reported previously (Platon et al. 2022). Regarding Gram-negative bacteria, which have higher resistance to antibiotics due to several factors, including having an outer membrane, which makes antibiotic diffusion inside the cell more difficult (Breijyeh et al. 2020). The findings of this research indicate higher diffusion of erythromycin nanocrystals inside the Gram-negative cell, which was observed by MIC reduction, where half of the MIC value was obtained by using nanocrystal (125 µg/ml

and 62.5 µg/ml against *P. aeruginosa* and *E. coli* respectively) in comparison with the erythromycin coarse drug (250 µg/ml and 125 µg/ml against *P. aeruginosa* and *E. coli* respectively), which was observed using the broth method. Using the agar diffusion essay for testing the effect of erythromycin and nanocrystal preparation of erythromycin didn't show any difference in activity, which might be due to the presence of agar in the media, which might affect the absorption of the drug in both formulations when compared with the broth method. Regarding Gram-positive bacteria used in this study, which were more susceptible to erythromycin (*B. cereus* and *S. aureus*) no significant enhancement of activity was recorded in both agar (agar well diffusion method) and MIC (broth method). These findings signify the importance of nanocrystal preparation for enhancing the susceptibility of Gram-negative bacteria to erythromycin.

The aerodynamic characteristics of inhaled powder are highly crucial. Powder deposition and distribution largely effect its efficacy and safety. Pulmonary targeted drug delivery includes controlling the quantity and the distribution of the drug. Aerodynamic particle size distribution (APSD) of inhaled products predicts deposition and distribution of the powder, which is fundamental for the development of inhaled powders (Yoshida et al. 2017). The previously reported dry powder inhalers had an ED% equal to or greater than 60% (Buttini et al. 2016). The reported nanocrystals in this work had a greater ED%, which indicates their suitability for powder inhalers. The induction, pre-separator, and the first tray in the NGI represent the extrathoratic part of the respiratory system. Trays from 2–7 represent the pulmonary system, whereas tray 8 represents the extrapulmonary system (Roberts and Mitchell 2016). The fine particle fraction of the emitted dose (FPF-ED) is the ratio between the fine particle mass and the emitted amount of the drug (Mehta, 2016). FPF-ED was determined by quantifying the nanocrystal amount in trays 2–7 divided by the emitted dose. This value is used to evaluate the deep deposition of the formulation in the lower respiratory tract (Tian et al. 2013). The commonly reported FPF% for marketed dry powder inhalers is equal to or higher than 20% (Buttini et al. 2016). However, the cumulative amount of erythromycin nanocrystals in trays 2–7 had an average of 16.37 ± 3.84 mg. In a previously reported study, erythromycin microspheres were formulated as a lung-targeting formulation. Their microspheres were made of gelatine and had an average size of 15.62 µm. Authors conducted an *in vivo* study on rats, which revealed that pulmonary erythromycin levels were 15.92 times higher than plasma (Fan et al. 2009). However, their study lacks the evaluation of microspheres exact deposition in the pulmonary system. The study did not show the aerodynamic behaviour of the microspheres in the pulmonary system. The oral form of erythromycin is available in 250 and 500 mg strengths; this antibiotic has a known low oral bioavailability that reaches 18% (Mather et al. 1981; Zeng et al. 2006; Papich 2016). Considering the latest, around 45 and 90 mg are the available erythromycins for systemic distribution. As reported above, MIC tests revealed that erythromycin nanocrystals had a significantly higher potency on *P.aeruginosa* and *E.coli* compared to erythromycin. The delivered erythromycin nanocrystals into deep trays (2–7) might be sufficient to inhibit bacterial growth. Further pharmacokinetic and pharmacodynamic *in vivo* studies on rats models are required to prove erythromycin nanocrystals efficacy on pulmonary infections. This study comes in parallel with several studies focusing on finding innovative formulations to deliver therapeutics *via* various routes of administration to enhance the therapeutic efficacy and minimise side effects while providing patients with convenient therapy (Abu Ershaid et al. 2023).

Conclusion

In conclusion, this study describes the formulation and characterisation of nanocrystal erythromycin for pulmonary delivery. This delivery approach represents a promising advancement in overcoming the limitations associated with oral erythromycin administration. The nanocrystals exhibited a significant reduction in particle size, leading to an increased surface area and improved drug solubility. These characteristics contribute to enhanced dissolution rates, crucial for effective pulmonary drug delivery. The formulation's efficient drug content, demonstrated by minimal use of excipients, further supports its potential as a robust alternative for erythromycin delivery. Moreover, the retained antibacterial activity of erythromycin in the nanocrystal formulation underscores its effectiveness against bacterial infections. The favourable aerodynamic performance suggests that this formulation has the potential to address challenges related to particle size and lung characteristics, providing a viable option for pulmonary administration. This research responds to the urgent need for improved antibiotic formulations, especially in the face of escalating bacterial resistance and challenges in developing new antibiotics. Further studies are needed to validate the efficacy and safety of this formulation, paving the way for its potential integration into clinical practice and addressing the pressing challenges in antibiotic therapy.

List of abbreviations

PDI: polydispersity index, **ED:** emitted dose, **MMAD:** mass median aerodynamic diameter, **MIC:** minimum inhibitory concentration, **FPF-ED:** fine particle fraction of emitted, **APSD:** aerodynamic particle size distribution, **CF:** cystic fibrosis, **SEM:** scanning electron microscope images, **NGI:** next generation impactor.

Acknowledgments

Authors wish to extend their sincere appreciation to Dr. Mike Haddad, who serves as the head of the innovation center at Isra University, Amman 11622, Jordan. The center generously granted open access to SEM, for which the authors are truly grateful.

References

Abadelah M, Al-Assadi J, Rooney J, Larhrib H (2020) The effect of inspiratory parameters after two separate inhalations on the dose emission of theophylline from low and high resistance dry powder inhalers. Saudi Pharmaceutical Journal 28(1): 74–86. https://doi.org/10.1016/j.jsps.2019.11.007

Abareshi A, Samadi N, Houshiar M, Nafisi S, Maibach HI (2021) Erythromycin dermal delivery by mos2 nanoflakes. Journal of Pharmaceutical Investigation 51(6): 691–700. https://doi.org/10.1007/s40005-021-00539-7

Abu Ershaid JM, Vora LK, Volpe-Zanutto F, Sabri AH, Peng K, Anjani QK, McKenna PE, Ripolin A, Larrañeta E, McCarthy HO, Donnelly RF (2023) Microneedle array patches for sustained delivery of fluphenazine: A micron scale approach for the management of schizophrenia. Biomaterials Advances 153: 213526. https://doi.org/10.1016/j.bioadv.2023.213526

Al-Tarawneh SF, Dahmash EZ, Alyami H, Abu-Doleh SM, Al-Ali S, Iyire A, Abuthawabeh R (2022) Mechanistic modelling of targeted pulmonary delivery of dactinomycin iron oxide-loaded nanoparticles for lung cancer therapy. Pharmaceutical Development and Technology 27(10): 1057–1068. https://doi.org/10.1080/10837450.2022.2152047

Asha BR, Goudanavar P, Koteswara Rao GSN, Gandla K, Raghavendra Naveen N, Majeed S, Muthukumarasamy R (2023) Qbd driven targeted pulmonary delivery of dexamethasone-loaded chitosan microspheres: Biodistribution and pharmacokinetic study. Saudi Pharmaceutical Journal 31(9): 101711. https://doi.org/10.1016/j.jsps.2023.101711

Balouiri M, Sadiki M, Ibnsouda SK (2016) Methods for in vitro evaluating antimicrobial activity: A review. Journal of Pharmaceutical Analysis 6(2): 71–79. https://doi.org/10.1016/j.jpha.2015.11.005

Bennabi L, Abedlmalek I, Ammari A, Sediri K, Bennabi F, Guemra K (2022) Synthesis and characterization of erythromycin loaded plga and pcl microspheres: Antimicrobial application. Microbial Biosystems 6(2): 43–52. https://doi.org/10.21608/mb.2022.122642.1051

Bhadra S, Prajapati AB, Bhadra D (2016) Development of ph sensitive polymeric nanoparticles of erythromycin stearate. Journal of Pharmacy & Bioallied Sciences 8(2): 135–140. https://doi.org/10.4103/0975-7406.171691

Breijyeh Z, Jubeh B, Karaman R (2020) Resistance of gram-negative bacteria to current antibacterial agents and approaches to resolve it. Molecules (Basel, Switzerland) 25(6): 1340. https://doi.org/10.3390/molecules25061340

Buttini F, Brambilla G, Copelli D, Sisti V, Balducci AG, Bettini R, Pasquali I (2016) Effect of flow rate on in vitro aerodynamic performance of nexthaler® in comparison with diskus® and turbohaler® dry powder inhalers. Journal of Aerosol Medicine and Pulmonary Drug Delivery 29(2): 167–178. https://doi.org/10.1089/jamp.2015.1220

Carter BL, Woodhead JC, Cole KJ, Milavetz G (1987) Gastrointestinal side effects with erythromycin preparations. Drug Intelligence & Clinical Pharmacy 21(9): 734–738. https://doi.org/10.1177/106002808702100914

Cheshmehnoor P, Rabbani S, Haeri A (2023) Quercetin nanocrystals prepared by a novel technique improve the dissolution rate and antifibrotic activity of quercetin. Nanomedicine 18(2): 89–107. https://doi.org/10.2217/nnm-2022-0032

Dave B, Emma L, Amanda B, Ann P, Saul NF (2012) Prescribing for children – taste and palatability affect adherence to antibiotics: A review. Archives of Disease in Childhood 97(3): 293. https://doi.org/10.1136/archdischild-2011-300909

Elsayed I, AbouGhaly MHH (2016) Inhalable nanocomposite microparticles: Preparation, characterization and factors affecting formulation. Expert Opinion on Drug Delivery 13(2): 207–222. https://doi.org/10.1517/17425247.2016.1102224

Essack S, Bell J, Burgoyne DS, Duerden M, Shephard A (2019) Topical (local) antibiotics for respiratory infections with sore throat: An antibiotic stewardship perspective. Journal of Clinical Pharmacy and Therapeutics 44(6): 829–837. https://doi.org/10.1111/jcpt.13012

Fan Y, Shan-Guang W, Yu-Fang P, Feng-Lan S, Tao L (2009) Preparation and characteristics of erythromycin microspheres for lung targeting. Drug Development and Industrial Pharmacy 35(6): 639–645. https://doi.org/10.1080/03639040802512243

Francino M (2016) Antibiotics and the human gut microbiome: Dysbioses and accumulation of resistances. Frontiers in Microbiology 6: 1543. https://doi.org/10.3389/fmicb.2015.01543

Gigliobianco MR, Casadidio C, Censi R, Di Martino P (2018) Nanocrystals of poorly soluble drugs: Drug bioavailability and physicochemical stability. Pharmaceutics 10(3): 134. https://doi.org/10.3390/pharmaceutics10030134

Gyselinck I, Janssens W (2024). Macrolide use in chronic obstructive pulmonary disease, Macrolides as immunomodulatory agents. Springer, 115–148. https://doi.org/10.1007/978-3-031-42859-3_6

He Y, Liang Y, Mak JCW, Liao Y, Li T, Yan R, Li H-F, Zheng Y (2020) Size effect of curcumin nanocrystals on dissolution, airway mucosa penetration, lung tissue distribution and absorption by pulmonary delivery. Colloids and Surfaces. B, Biointerfaces 186: 110703. https://doi.org/10.1016/j.colsurfb.2019.110703

Heijerman H (2005) Infection and inflammation in cystic fibrosis: A short review. Journal of Cystic Fibrosis 4: 3–5. https://doi.org/10.1016/j.jcf.2005.05.005

Hoyt JC, Robbins RA (2001) Macrolide antibiotics and pulmonary inflammation. FEMS Microbiology Letters 205(1): 1–7. https://doi.org/10.1111/j.1574-6968.2001.tb10917.x

Jiang T, Han N, Zhao B, Xie Y, Wang S (2012) Enhanced dissolution rate and oral bioavailability of simvastatin nanocrystal prepared by sono-precipitation. Drug Development and Industrial Pharmacy 38(10): 1230–1239. https://doi.org/10.3109/03639045.2011.645830

Jin S (2024). Pseudomonas aeruginosa, Molecular medical microbiology. Elsevier, 811–825. https://doi.org/10.1016/B978-0-12-818619-0.00064-2

Jin N, Pyo S M, Keck C, and Müller R (2019) Azithromycin nanocrystals for dermal prevention of tick bite infections. Die Pharmazie-An international journal of pharmaceutical sciences 74(5): 277–285.

Kanfer I, Skinner MF, Walker RB (1998) Analysis of macrolide antibiotics. Journal of Chromatography A 812(1): 255–286. https://doi.org/10.1016/S0021-9673(98)00276-3

Kar A, Mukherjee SK, Barik S, Hossain ST (2024) Antimicrobial activity of trigonelline hydrochloride against pseudomonas aeruginosa and its quorum-sensing regulated molecular mechanisms on biofilm formation and virulence. ACS Infectious Diseases. https://doi.org/10.1021/acsinfecdis.3c00617

Khatib I, Khanal D, Ruan J, Cipolla D, Dayton F, Blanchard JD, Chan H-K (2019) Ciprofloxacin nanocrystals liposomal powders for controlled drug release via inhalation. International Journal of Pharmaceutics 566: 641–651. https://doi.org/10.1016/j.ijpharm.2019.05.068

Kim N, Duncan GA, Hanes J, Suk JS (2016) Barriers to inhaled gene therapy of obstructive lung diseases: A review. Journal of Controlled Release 240: 465–488. https://doi.org/10.1016/j.jconrel.2016.05.031

Kulshreshtha AK, Singh ON, Wall GM (2009) Pharmaceutical suspensions. In: Kulshreshtha AK, Singh ON, Wall GM (Eds) From formulation development to manufacturing: Springer. https://doi.org/10.1007/978-1-4419-1087-5

Ling X, Shen Y, Sun C, Tu J (2014) Current progress on pulmonary drug delivery. Journal of Pharmacy Research 33: 711–713.

Liu F, Park JY, Zhang Y, Conwell C, Liu Y, Bathula SR, Huang L (2010) Targeted cancer therapy with novel high drug- loading nanocrystals. Journal of Pharmaceutical Sciences 99(8): 3542–3551. https://doi.org/10.1002/jps.22112

Liu Y, Liu W, Xiong S, Luo J, Li Y, Zhao Y, Wang Q, Zhang Z, Chen X, Chen T (2020) Highly stabilized nanocrystals delivering ginkgolide b in protecting against the parkinson's disease. International Journal of Pharmaceutics 577: 119053. https://doi.org/10.1016/j.ijpharm.2020.119053

Liu J, Chen Q-X, Wu W-F, Wang D, Zhao S-Y, Li J-H, Chang Y-Q, Zeng S-G, Hu J-Y, Li Y-J (2024) Novel ligustilide derivatives target quorum sensing system lasr/lasb and relieve inflammatory response against pseudomonas aeruginosa infection. European Journal of Medicinal Chemistry 263: 115972. https://doi.org/10.1016/j.ejmech.2023.115972

Loira-Pastoriza C, Todoroff J, Vanbever R (2014) Delivery strategies for sustained drug release in the lungs. Advanced Drug Delivery Reviews 75: 81–91. https://doi.org/10.1016/j.addr.2014.05.017

Lozano-Iturbe V, Blanco-Agudín N, Vázquez-Espinosa E, Fernández-Vega I, Merayo-Lloves J, Vazquez F, Girón RM, Quirós LM (2024) The binding of pseudomonas aeruginosa to cystic fibrosis bronchial epithelial model cells alters the composition of the exosomes they produce compared to healthy control cells. International Journal of Molecular Sciences 25(2): 895. https://doi.org/10.3390/ijms25020895

Mangal S, Gao W, Li T, Zhou QT (2017) Pulmonary delivery of nanoparticle chemotherapy for the treatment of lung cancers: Challenges and opportunities. Acta Pharmacologica Sinica 38(6): 782–797. https://doi.org/10.1038/aps.2017.34

Mansour HM, Rhee Y-S, Wu X (2009) Nanomedicine in pulmonary delivery. International Journal of Nanomedicine 4: 299–319. https://doi.org/10.2147/IJN.S4937

Marple VA, Roberts DL, Romay FJ, Miller NC, Truman KG, Van Oort M, Olsson B, Holroyd MJ, Mitchell JP, Hochrainer D (2003) Next generation pharmaceutical impactor (a new impactor for pharmaceutical inhaler testing). Part i: Design. Journal of Aerosol Medicine 16(3): 283–299. https://doi.org/10.1089/089426803769017659

Mather L, Austin K, Philpot C, McDonald P (1981) Absorption and bioavailability of oral erythromycin. British Journal of Clinical Pharmacology 12(2): 131–140. https://doi.org/10.1111/j.1365-2125.1981.tb01191.x

Mehta P (2016) Dry powder inhalers: A focus on advancements in novel drug delivery systems. Journal of Drug Delivery, 2016. https://doi.org/10.1155/2016/8290963

Müller RH, Gohla S, Keck CM (2011) State of the art of nanocrystals – special features, production, nanotoxicology aspects and intracellular delivery. European Journal of Pharmaceutics and Biopharmaceutics 78(1): 1–9. https://doi.org/10.1016/j.ejpb.2011.01.007

Mushtaq RY, Naveen NR, Tiyyagura P, Hosny KM, Alahmadi AA, Majrashi MA, Mamidipalli NR, Safhi AY, Alissa M, Sabei FY (2024) Development, optimization and in-vivo pharmacokinetic evaluation of flubiprofen nanocrystal tablets for efficient chronotherapy against rheumatoid arthritis. Journal of Drug Delivery Science and Technology 91: 105240. https://doi.org/10.1016/j.jddst.2023.105240

Pandey R, Ahmad Z (2011) Nanomedicine and experimental tuberculosis: Facts, flaws, and future. Nanomedicine; Nanotechnology, Biology, and Medicine 7(3): 259–272. https://doi.org/10.1016/j.nano.2011.01.009

Papich MG (2016) Erythromycin. In: Papich MG (Ed.) Saunders handbook of veterinary drugs (4th edn.). St. Louis: W.B. Saunders, 297–299. https://doi.org/10.1016/B978-0-323-24485-5.00247-3

Park H, Park H, Na K (2015) Dual propionibacterium acnes therapy using skin penetration-enhanced liposomes loaded with a photosensitizer and an antibiotic. Journal of Porphyrins and Phthalocyanines 19(08): 956–966. https://doi.org/10.1142/S1088424615500686

Parkins MD, Somayaji R, Waters VJ (2018) Epidemiology, biology, and impact of clonal pseudomonas aeruginosa infections in cystic fibrosis. Clinical Microbiology Reviews 31(4). https://doi.org/10.1128/CMR.00019-18

Patton JS, Byron PR (2007) Inhaling medicines: Delivering drugs to the body through the lungs. Nature Reviews. Drug Discovery 6(1): 67–74. https://doi.org/10.1038/nrd2153

Pelikh O, Eckert RW, Pinnapireddy SR, Keck CM (2021) Hair follicle targeting with curcumin nanocrystals: Influence of the formulation properties on the penetration efficacy. Journal of Controlled Release 329: 598–613. https://doi.org/10.1016/j.jconrel.2020.09.053

Platon V-M, Dragoi B, Marin L (2022) Erythromycin formulations—A journey to advanced drug delivery. Pharmaceutics 14(10): 2180. https://doi.org/10.3390/pharmaceutics14102180

Roberts DL, Mitchell J (2016) The next generation impactor (ngi™)–manufacturing control: Part ii. Collection cups and the critical jet-to-plate distance. City: Inhalation.

Siow CRS, Heng PWS, Chan LW (2018) Bulk freeze-drying milling: A versatile method of developing highly porous cushioning excipients for compacted multiple-unit pellet systems (mups). AAPS PharmSciTech 19: 845–857. https://doi.org/10.1208/s12249-017-0899-6

Tian G, Longest PW, Li X, Hindle M (2013) Targeting aerosol deposition to and within the lung airways using excipient enhanced growth. Journal of Aerosol Medicine and Pulmonary Drug Delivery 26(5): 248–265. https://doi.org/10.1089/jamp.2012.0997

Wang Z, Wang J, Zhang M, Dang L (2006) Solubility of erythromycin a dihydrate in different pure solvents and acetone + water binary mixtures between 293 k and 323 k. Journal of Chemical & Engineering Data 51(3): 1062–1065. https://doi.org/10.1021/je0505265

Xiang H, Xu S, Li J, Li Y, Xue X, Liu Y, Li J, Miao X (2022) Functional drug nanocrystals for cancer-target delivery. Journal of Drug Delivery Science and Technology 76: 103807. https://doi.org/10.1016/j.jddst.2022.103807

Yoshida H, Kuwana A, Shibata H, Izutsu K-i, Goda Y (2017) Comparison of aerodynamic particle size distribution between a next generation impactor and a cascade impactor at a range of flow rates. AAPS PharmSciTech 18(3): 646–653. https://doi.org/10.1208/s12249-016-0544-9

Yue P, Zhou W, Huang G, Lei F, Chen Y, Ma Z, Chen L, Yang M (2022) Nanocrystals based pulmonary inhalation delivery system: Advance and challenge. Drug Delivery 29(1): 637–651. https://doi.org/10.1080/10717544.2022.2039809

Yue P-f, Liu Y, Xie J, Chen Y-c, Yang M (2018) Review and prospect on preparation technology of drug nanocrystals in the past thirty years. Acta Pharmaceutica Sinica, 529–537.

Zeng GX, Zhong GP, Wang XD, Huang L H, Huang M (2006) Bioavailability and bioequivalence of erythromycin ethylsuccinate granules in healthy volunteers. Chinese journal of infection and chemotherapy 6(4): 228–230.

Zhu Y, Fu Y, Zhang A, Wang X, Zhao Z, Zhang Y, Yin T, Gou J, Wang Y, He H (2022) Rod-shaped nintedanib nanocrystals improved oral bioavailability through multiple intestinal absorption pathways. European Journal of Pharmaceutical Sciences 168: 106047. https://doi.org/10.1016/j.ejps.2021.106047